Capacitance: A property of nanoscale materials based on spatial symmetry of discrete electrons

Tim LaFave Jr.

Department of Physics and Astronomy, University of Iowa, Iowa City, IA 55242, USA

Raphael Tsu

Department of Electrical Engineering, University of North Carolina, Charlotte, NC 28223, USA

Abstract

Capacitance is a measure of the ability to store electrons and is conventionally considered to be a constant dependent upon the shape of metal contacts and the dimensions of the system. In general, however, equipotentials of dielectric systems without metal contacts take the shape of very complex three-dimensional surfaces resulting from the spatial distribution of discrete electrons. The fundamental definition of capacitance, $C \equiv Q/V$, in which V is the potential within which electrons are confined, requires that the total capacitance take into account local capacitances of every electron and all cross-capacitances. To circumvent this complexity, the average total electrostatic potential experienced by each electron is utilized to obtain a capacitance expression generally appropriate to dielectric systems consisting of few excess electrons without metallic contacts. The capacitance may then be expressed as an exact function of the total electrostatic potential energy of the system. The integrity of this expression is demonstrated using a representative system of N excess electrons confined to a dielectric sphere. The capacitance expression is shown to be consistent with the conventional capacitance for a single electron dielectric sphere and with $C = 4\pi\varepsilon_0\varepsilon' a$ for metallic spheres. A relatively large sphere size is chosen such that the magnetic moment interaction energy is negligibly small. The capacitance exhibits a non-uniform relationship with respect to N coincident with shell-filling patterns of the natural atomic system. This classical electrostatic interactions approach is particularly appealing to the practical development of nanoscale materials and devices as it circumvents immediate recourse to often unintuitive and complicated quantum mechanical descriptions.

Cite as: T. LaFave Jr. & R. Tsu *Microelectron. J.* **39** 617-623 (2008). DOI: 10.1016/j.mejo.2007.07.105

1. Introduction

The characterization of phenomena resulting from the confinement of few electrons is central to the design and development of current and near-future nanoscale materials. We recently demonstrated variation of the classical capacitance of dielectric spheres with the number of stored electrons[1]a result encouraging further exploration of classical electrostatic phenomena. Conventionally, capacitance is measured as a function of the potential difference between two metal contacts. Isolated dielectric systems, however, function in the absence of well-defined equipotential surfaces. Instead, equipotentials take the shape of very complex three-dimensional surfaces resulting from the spatial distribution of stored electrons.

We derive a time-independent, electrostatic capacitance expression for dielectric systems in the absence of metallic contacts[2] based on the fundamental capacitance definition, $C \equiv Q/V$. The confining potential, V, conventionally given as the potential difference between two metal surfaces is replaced by the average electrostatic potential experienced locally by each electron. The integrity of the proposed capacitance expression is validated by numerical agreement with the conventional capacitance for singleelectron dielectric spheres and the constant conventional capacitance of metallic spheres. In the former case, the two models should agree as the single electron system represents a per-

Email address: tjlafave@yahoo.com (Tim LaFave Jr.)

Preprint accepted by Elsevier for publication in Microelectronics Journal. *Prepared: November 27, 2013*

fect spherical symmetry in which the charge may be represented by a single point charge at the origin or as a uniform surface charge.

The addition or removal of an electron to or from a dielectric sphere represents capacitance changes. When compared with neighboring capacitance states, a broad trend among even and odd number states of electrons emerges. With this observation, each N electron system is proposed to be treated as a distinct phase characterized by its unique range of spatial electron symmetries, in order to properly facilitate the development of capacitance studies. In particular, electrostatic, time-independent parameters of a given N electron system are considered *monophasic*, while parametric variations that occur without electron loss or gain may be characterized by *intraphasic* parameters. Parametric variations resulting from electron loss or gain may then be characterized by *interphasic* parameters. The conventional capacitance does not provide for characterization of intraphasic phenomena. The discrete charge dielectric (DCD) model presented here, however, exposes a vibrant intraphasic range of complexity inherent to isolated nanoscale systems.

2. The DCD model

The DCD model is very practical and intuitive, consisting of a uniform dielectric sphere of permittivity ε and radius a surrounded by a uniform dielectric medium of lesser permittivity, ε_0. The dielectric function is assumed to change abruptly at r a. For the purpose of illustration, a sphere of radius $a = 10$nm, $\varepsilon = 12$ and $\varepsilon' = 4$, is chosen such that magnetostatic interaction energy ($\leq 5 \times 10^{-8}$ eV for $N = 30$ electrons) arising from the magnetic moments of electrons is negligible compared to the total electrostatic interaction energy ($\sim$ 30eV for $N = 30$). For atom-size systems ($a \sim 0.1$nm), however, the magnetostatic interaction becomes significant (≤ 0.3eV for $N = 30$).

Since the dielectric constant of the sphere is greater than the permittivity of the surrounding medium, electrons in the sphere induce a net-negative surface charge. Each electron stored in the dielectric sphere interacts with electrostatic potentials due to all other electrons and induced surface charges. These interactions may be placed in three categories: (1) polarizations with surface charges induced by other electrons, (2) self-polarizations with the surface charge induced by each electron itself, and (3) Coulomb interactions with other electrons. The first two result from electron interactions with the potential solutions of Poissons equation resulting from polarized surface charges[3]

$$\phi(r_i,r_j)=\frac{q}{4\pi\varepsilon_0\varepsilon a}\sum_{l=0}^{\infty}\frac{(\varepsilon-\varepsilon')(l+1)}{[\varepsilon'+l(\varepsilon+\varepsilon')]}\frac{r_i^l r_j^l}{a^{2l}}P_l[\cos(\gamma_{ij})], \quad (1)$$

where r_i is the source point, r_j is the field point, and $P_l(\cos\gamma_{ij})$ are Legendre polynomials for each angle γ_{ij} subtended by $\vec{r}_i$ and $\vec{r}_j$.

A special case of the DCD model is the presence of a single excess electron in a dielectric sphere. The total electrostatic interaction energy of the electron is given by

$$E_S(r_i) = e\phi(r_i) - W$$

with

$$W=\int_0^e \phi(r_i)\mathrm{d}q$$
$$= \frac{e^2}{8\pi\varepsilon_0\varepsilon a}\sum_{l=0}^{\infty}\frac{(\varepsilon-\varepsilon')(l+1)}{\varepsilon'+l(\varepsilon+\varepsilon')]}\left(\frac{r_i}{a}\right)^{2l}=\frac{e\phi(r_i)}{2},$$

valid for all $r_i < a$, is the net work done in polarizing the dielectric sphere. Here, integration over charge is appropriate as polarization results in an infinitely divisible surface charge. Note that for self-polarizations $r_i = r_j$ in Eq. 1. Consequently, the self-polarization energy is

$$E_s(r_i) = \frac{1}{2}e\phi(r_i). \quad (2)$$

A factor of 1/2 appears in Eq. 2 as an explicit consequence of having subtracted the work done by the electron to polarize an infinitely divisible net surface charge at the dielectric interface rather than simply due to arguments of this interaction being a self-interaction[4]. The interaction energy must only account for the interaction of the electron with the potential at r_i.

Having minimized the self-polarization energy, the electron is intuitively found at the center of the sphere. Equilibrium configurations of N-electron systems resulting from minimization of the total interaction energy, as described previously[1,2], are found to be solutions of the single-shell Thomson problem[5–17] with electron radii, $b < a$. The Thomson problem has been widely studied, accurate solutions of which have emerged in the past two decades for large values of N.

3. Monophasic capacitance

The fundamental capacitance definition, $C \equiv Q/V$, represents the total free charge, $Q \equiv Ne$, confined by a total potential, V. Only confined excess electrons contribute to the total charge, Q. The polarized surface charge is implicitly taken into account by the potential, Eq. 1. The ideal charge configurations of the conventional model, a point charge at the origin or an infinitely divisible surface charge, produce spherical equipotentials that conform to the shape of the sphere. In the DCD model, however, equipotentials take the form of complicated three-dimensional surfaces. In general, the potential with which each electron interacts varies from site to site. An equivalent system capacitance may be constructed by summing all the local *electrophasic* capacitances of each electron in series or parallel; however, proper evaluation of cross-capacitances among regions is formidable. Therefore, it is appropriate to express the system capacitance using the average total potential experienced by each electron,

$$\bar{V}_{\mathrm{TOT}}(r_i) = \frac{1}{N}\sum_{i=1}^{N}\phi_i(r_i) = \frac{V(N)}{N}$$

yielding the definition of *monophasic* capacitance,

$$C(N) \equiv \frac{Q}{\bar{V}_{\mathrm{TOT}}(r_i)} = N\frac{Q}{V(N)}. \tag{3}$$

The scalar electrostatic potential is the sum of all component potentials,

$$V(N) = \phi_C(N) + \phi_P(N) + \phi_S(N).$$

The conventional capacitance of an isolated dielectric sphere may be expressed by

$$C(\varepsilon) = \frac{Q^2}{2E(\varepsilon)} \tag{4}$$

with the conventional energy given by

$$E(\varepsilon) = \frac{Q^2}{8\pi\varepsilon_0 a}\left(\frac{1}{\varepsilon'} - \frac{1}{\varepsilon}\right). \tag{5}$$

Evaluation of the monophasic capacitance, Eq. 3, for $\varepsilon = 12, 24, 120$ and 1200 for a sphere of radius 10nm with $\varepsilon' = 4$ numerically agrees with Eq. 4 for $N = 1$ (Fig. 1). The monophasic capacitance given by the DCD model converges to the constant conventional capacitance of a metallic sphere, $C = 4\pi\varepsilon_0\varepsilon' a$, as ε grows very large (Fig. 1). Based purely upon a fundamental definition, the monophasic capacitance represents a significant improvement upon our previous capacitance for discrete electron systems[1].

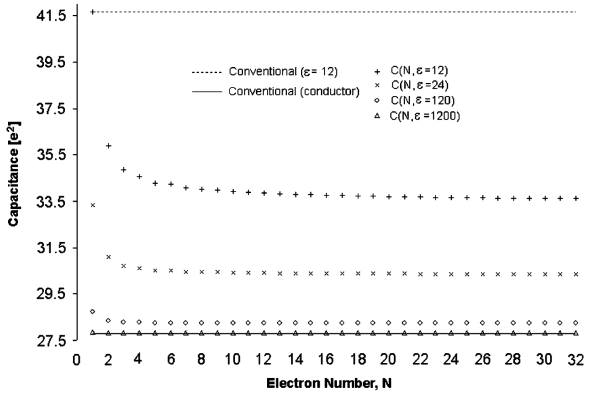

Figure 1: Comparison of monophasic capacitance with conventional values. The monophasic capacitance, $C(N) \equiv Ne/V(N)$, converges to the conventional capacitance, $C = 4\pi\varepsilon_0\varepsilon' a$, of a conducting sphere for large dielectric constant and in general for $N = 1$. Here, $a = 10$nm and $\varepsilon' = 4$

4. Interphasic phenomena

As a rule of thumb, the addition of an electron to the sphere lowers the capacitance as the sphere loses capacity for additional electrons. However, results of the DCD model demonstrate that lower spatial symmetry corresponds to lower monophasic capacitance. A comparison of interphasic capacitance differences, $\delta C = |C(N) - C(N-1)| - |C(N) - C(N+1)|$, yields a trend of monophasic capacitances for even $[N]$ phases, shown in Fig. 2a, that are closer in value to the monophasic capacitance of neighboring $[N-1]$ phases than to $[N+1]$ phases. Consequently, even-N phases tend to have greater capacity for an additional electron than odd-N phases, indicating that even-N phases lie lower in energy than odd-N phases. Indeed, a plot of interphasic energy differences (Fig. 2b) also clearly bears out this resulting even/odd trend.

Symmetry differences between neighboring phases may be directly studied. For example, the interphasic capacitance difference $\Delta C^{+}(N) = C(N) - C(N+1)$ represents capacitance loss for each $[N]$ electron phase with the addition of an electron. This interphasic capacitance yields pronounced non-uniformities as shown in Fig. 3. When an electron is removed from an $[N+1]$ phase, the resulting $[N]$ phase has a greater capacity for electrons. Thus, $\Delta C + (N)$, is generally positive and diminishes as N becomes very large as expected. Smaller differences indicate closer proximity of odd-N capacitances to neighboring $[N+1]$ phases.

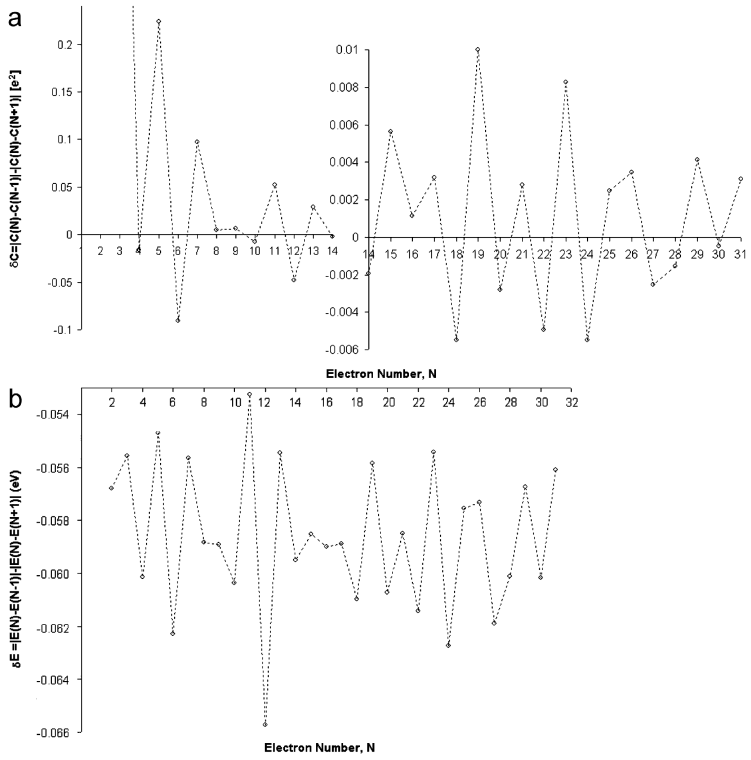

Figure 2: Interphasic differences. (a) Interphasic capacitance differences, indicate a broad trend of lower even-N phases representing monophasic capacitance states lying closer to the preceding $[N-1]$ phase than the neighboring $[N+1]$ phase. These lower values represent phases with greater electrostatic capacity than odd-N phase values. The vertical scale is magnified to accentuate features for $N \geq 14$. (b) Interphasic energy differences, also exhibit even-numbered phase energies lying closer to preceding $[N-1]$ phases than neighboring $[N+1]$ phases, indicating greater even-N symmetries. Note the trend reversal in the region $24 < N < 29$ for both capacitance and energy.

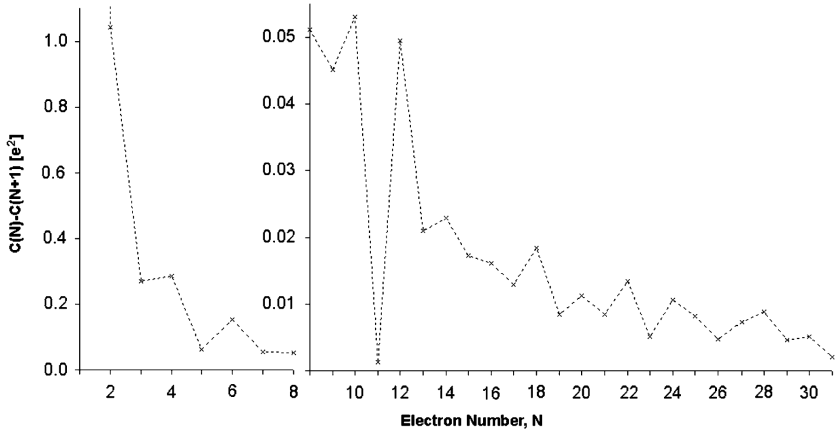

Figure 3: Interphasic capacitance $\Delta C^{+}(N) = C(N) - C(N+1)$. The interphasic capacitance associated with electron addition indicates a trend of greater capacity losses associated with odd-N phases than even-N phases. The vertical scale is magnified to accentuate features for $N \geq 8$.

5. Intraphasic phenomena

To examine parametric variations exclusively associated with electron symmetry, it is necessary to hold fixed the total charge (number of electrons) in the system. To examine one such intraphasic variation, consider the symmetry change involved in the process of moving an electron from a particular equilibrium $[N]$ configuration to the center of the sphere. The electron moved to the origin contributes to the perfect spherical symmetry of the system while the remaining $N-1$ electrons form an $[N-1]$ symmetry about the origin. The resulting $[N-1, 1\mathrm{e}]$ configuration has symmetry identical to the $[N-1]$ phase without an electron at the origin. The process described may be considered a symmetric loss of an electron from the sphere just as the conventional electrostatic image of an electrons charge is moved to infinity. The amount of work required to perform this symmetry change may be evaluated within the DCD model and is collected in Fig. 4a for each $[N]$ phase from which an $[N-1, 1\mathrm{e}]$ configuration is obtained (that is, an $N-1$ electron symmetry with one electron at the origin). The conventional model inadequately provides for no work done in this process, as the total charge on the system is unchanged.

The symmetric loss of an electron is the equivalent of ionizing a single electron from the system. Indeed, utilizing only Coulomb interaction components of the total energy, reducing electron radii to quantum mechanical radii[18], and assuming the permittivity of free space, ε_0, a plot of these energies (Fig. 4b) bears a striking resemblance to a plot of empirical ionization energies[19] of neutral atoms (Fig. 4c). Similarities among inter-period energy trends are noted including rising outer p-shell energies and the wavy trend of outer d-shell energies. The DCD model yields energies comparably larger than established ionization energies, owing to assumptions of permittivity and atom size that may later be treated as variational parameters within a broader classical theory.

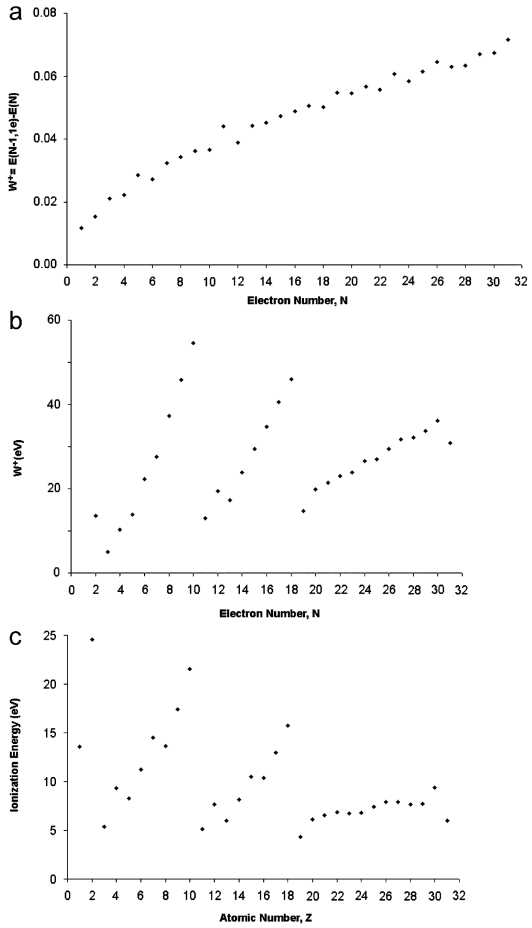

Figure 4: Intraphasic energy. (a) $W^+ = E(N-1, 1\mathrm{e})$ due to *symmetric loss* of an electron. Note that non-uniformities coincident with electron shell changes in the natural atomic structure. (b) Using quantum mechanical radii and $\varepsilon = \varepsilon_0$, coincides with (c) known ionization energies of neutral atoms.

6. Electrostatic shell-filling

Non-uniformities in Fig. 4a are uniquely coincident with abrupt differences in electron shell symmetries of the atomic structure. The larger differences at $N = 3, 5, 11$, and 19, for example, are coincident with the start of new electron shells associated with elements having atomic numbers $Z = 3$ (Li), $Z = 5$ (B), $Z = 11$ (Na), and $Z = 19$ (K), respectively. These electrostatic non-uniformities represent parametric shifts due to spatial symmetry changes between 1s and 2s shells, 2s and 2p shells, 2p and 3s shells, and so forth. Interestingly, the region in which the even/odd trend is violated in Fig. 2 ($24 < N < 29$) is bounded by $Z = 24$ (Cr) and $Z = 29$ (Cu) which have half-filled 4s shells that violate Hunds rule of shell-filling, for example. The non-uniformity at $N = 21$ is not as pronounced as others, perhaps owing to the proximity of the 3d energy to 4s energy. Within the DCD model, the close proximity of energies is demonstrably a consequence of similar spatial symmetries. As well, each period ends ($N = 2, 10$, and 18) with ener-

gies that tend to be lower than the general trend as do filled p-shells of noble elements that have low ground state energies.

7. Discussion and comments

From a purely classical electrostatic foundation, the DCD model provides a rich and vibrant range of phenomena of particular interest to the nanoscale science of confined charge systems. Among the primary results obtained using this model, much emphasis is placed on the symmetry of collections of discrete electrons. Consequently, the model is based on the discrete, rather than the wave, nature of electrons characteristic of classical mechanics. The model is highly intuitive, practical and computationally efficient as it draws upon well-established electrostatic principles appropriately applied to satisfy the necessary boundary conditions of nanoscale materials as opposed to assumptions made with continuum and periodic systems as often found in solid state theories.

Indeed, as solutions of the established single-shell Thomson problem are obtained in this work, some resulting trends are readily verified using numerical solutions found in the literature[7,10]. However, such solutions only involve Coulomb interaction energies among electrons on a fictitious unit sphere and any mechanism to appropriately vary the size of each system. Here, we have chosen to minimize the total interaction energy of electron ensembles within a dielectric sphere model to include polarization interactions. Furthermore, only here is a classical electrostatic identification made with the periodic table of elements for which the Thomson problem was originally proposed[5] in 1904 through inherent symmetry properties of discrete electrons confined to a spherical system. Thus, we have presented a valid extension of the classical Thomson model of the atom. From a broad perspective, the atomic system is a collection of electrons constrained to a spherical spatial symmetry. The similar symmetries of the atomic and dielectric systems allows us to conclude that inter-shell energy differences derive from classical electrostatic solutions of Poissons equation in the time-independent domain which represent salient features of the time-dependent Schrödinger equation.

A useful component of the DCD model is the proposed monophasic capacitance as it is directly proportional to spatial electron symmetry. Greater symmetry corresponds to greater capacitance owing to lower electrostatic energy. The monophasic capacitance represents an improvement over existing expressions as it bears out, and is substantiated by, unique correspondences with natural atomic systems and has been shown to result in an even/odd trend unprecedented in any classical model. The latter feature substantiates our proposed argument to treat each Nelectron system as a distinct phase characterized by its unique range of spatial symmetry properties.

Parametric, time-dependent changes within a phase, however, such as intraphasic capacitances, should be born out in detail by any electrodynamic model utilizing differential capacitances, for example, $C_d = \mathrm{d}Q/\mathrm{d}V$ in the range of possible $\mathrm{d}V$ when $\mathrm{d}Q = 0$. A rapid interphasic transition may be represented by $C_\Delta = \Delta Q/\Delta V$ in which the rapid change in charge may be well approximated by $\Delta Q \to e$. Alternatively, slow phase transitions may be represented by the differential $C_d = \mathrm{d}Q/\mathrm{d}V$ as $\mathrm{d}Q \to 0$. Characterization of interphasic phenomena is governed by the dynamics of each phase transition, details of which are not contained in time-dependent capacitance models in the literature[4,20–22].

Continued usefulness of the DCD model depends upon utilization and understanding of underlying spatial symmetry properties from which all physical properties derive as hinted by the usefulness of density functionals that replace the role of wavefunctions in conventional quantum mechanics. As well, a Jellium-like model may be constructed to account for the difference of net-charge between the atomic and dielectric systems. The non-uniformity of induced surface charges in the DCD model is a reflection of internal Thomson electron geometries. However, distributions of protons in atomic nuclei that create the potential well in which electrons are confined are also not spherically uniform.

The dielectric boundary of our model is chosen as a sharp interface for the purpose of illustration, providing a specific system size whereas no true boundary exists in atomic systems from which inside and outside may be rigidly defined. The maxima of quantum mechanical probability distributions, $\Psi^*\Psi$, are typically used as atomic radii. The key to the single-shell Thomson model is use of the electron radius as a fitting parameter just as the monophasic spatial symmetry is independent of electron radius. Here, capacitance is strictly defined within the volume of the entire sphere while it is conventionally defined per unit length or unit vol-

ume within a much broader system. An enhanced DCD model with variable radius may be developed to overcome obstacles associated with system size for direct comparison with the periodic table of elements and for use with a variety of nanoscale systems.

The DCD model provides a better understanding of design and performance issues associated with small nanoelectronic devices that operate in a regime of negligible magnetic interactions and provides for details of current and near-future measurements not possible in conventional classical models. A magnetostatic component may be developed to complement the DCD model that may provide an even richer model of atomic and nanoscale phenomena.

A new classical-quantum theory may emerge that more closely resembles density functional theory[23–25] than standard quantum mechanics as the spatial symmetry properties of discrete charges is here shown to play a significant role. Both DFT and quantum mechanics rely upon solutions of the Schrödinger equation while here a classical connection to atomic shell filling by solutions of the Poisson equation has been demonstrated. The DCD model provides a richly detailed description of timeindependent phenomena of nanoscale electronic, biological and chemical systems in use today and the near future.

References

[1] J. Zhu, T. LaFave Jr., R. Tsu, Classical capacitance of few-electron dielectric spheres, Microelectron. J. 37 (2006) 1293-1296.

[2] T. LaFave Jr., The classical electrostatic periodic table, capacitance of few electron dielectric spheres and a novel treatment of one- and two-electron finite quantum wells. Ph.D. Dissertation, University of North Carolina, Charlotte, 2006.

[3] C. J. F. Böttcher, Theory of Electric Polarization, vol. I: Dielectrics in Static Fields, Elsevier, Amsterdam, 1973.

[4] D. Babić, R. Tsu, R. F. Greene, Ground-state energies of one- and two-electron silicon dots in an amorphous silicon dioxide, Phys. Rev. B 45 (1992) 1415014155.

[5] J. J. Thomson, On The Structure of the Atom, Philos. Mag. 7 (1904) 237.

[6] J. J. Thomson, The Electron in Chemistry, Franklin Institute, Philadelphia, 1923.

[7] S. Bednarek, B. Szafran, J. Adamowski, Many-electron artificial atoms, Phys. Rev. B 59 (1999) 13036.

[8] T. Erber, G. M. Hockney, Equilibrium configurations of N equal charges on a sphere, J. Phys. A 24 (1991) L1369-L1377.

[9] J. R. Edmundson, The distribution of point charges on the surface of a sphere, Acta Crystallogr. A 49 (1992) 60-69.

[10] L. Glasser, A. G. Every, Energies and spacings of point charges on a sphere, J. Phys. A 25 (1992) 2473.

[11] E. L. Altschuler, T. J. Williams, E. R. Ratner, F. Dowla, F. Wooten, Method of constrained global optimization, Phys. Rev. Lett. 74 (1995) 2671-2674.

[12] T. Erber, G. M. Hockney, Comment on method of constrained global optimization, Phys. Rev. Lett. 74 (1995) 1482.

[13] E. L. Altschuler, T. J. Williams, E. R. Ratner, F. Dowla, F. Wooten, E. L. Altchuler, et al., Reply. Phys. Rev. Lett. 74 (1995) 1483.

[14] J. R. Morris, D. M. Deaven, K. M. Ho, Genetic-algorithm energy minimization for point charges on a sphere, Phys. Rev. B 53 (1996) R1740.

[15] J. R. Edmundson, The arrangement of point charges with tetrahedral and octahedral symmetry on the surface of a sphere with minimum Coulombic potential energy, Acta Crystallogr. A 49 (1997) 648-654.

[16] E. L. Altschuler, A. Perez-Garrido, Global minimum for Thomsons problem of charges on a sphere, Phys. Rev. E 71 (2005) 047703.

[17] S. Smale, Mathematical problems for the next century, Math. Intell. 20 (1998) 7.

[18] Periodic Table of Elements, Sargent-Welch Sci. Co. Cat.# S-18806, 1979.

[19] Ionization energies of neutral atoms, `http://www.nist.gov/pml/data/ion_energy.cfm`.

[20] M. Macucci, K. Hess, J. G. Iafrate, Electronic energy spectrum and the concept of capacitance in quantum dots, Phys. Rev. B 48 (1993) 17354.

[21] G. J. Iafrate, K. Hess, J. B. Krieger, M. Macucci, Capacitive nature of atomic-sized structures, Phys. Rev. B 52 (1995) 10737.

[22] M. Macucci, K. Hess, J. G. Iafrate, Simulation of electronic properties and capacitance of quantum dots, J. Appl. Phys. 77 (1995) 7.

[23] P. Hohenberg, W. Kohn, Inhomogeneous electron gas, Phys. Rev. 136 (1964) B864-B871.

[24] W. Kohn, L. J. Sham, Self-consistent equations including exchange and correlation effects, Phys. Rev. 140 (1965) A1133-A1138.

[25] W. Kohn, Nobel lecture: electronic structure of matterwave functions and density functionals, Rev. Mod. Phys. 71 (1999) 1253-1266.